http://journal.uir.ac.id/index.php/JGEET

E-ISSN : 2541-5794
P-ISSN : 2503-216X

Journal of Geoscience,
Engineering, Environment, and Technology
Vol 9 No 2 2024

RESEARCH ARTICLE

Tsunami Modeling Using DEMNAS and DEM Data from UAV Surveys for Planning Evacuation Routes on Samas Coast, Bantul Regency

Sulpisius Sihombing[1], Sudarmaji[1*], Bambang Sunardi[2], Herlan Darmawan[1]

[1] *Faculty of Mathematics and Natural Sciences, Gadjah Mada University, Yogyakarta, Indonesia.*
[2] *Meteorology, Climatology, and Geophysical Agency, Yogyakarta, Indonesia.*

* Corresponding author: ajisaroji@ugm.ac.id
Tel.: Tel.:+62-81392840341; fax: +62-274-545183
Received: Nov 26, 2023; Accepted: May 22, 2024.
DOI: 10.25299/jgeet.2024.9.2.14777

Abstract

The interaction between the Indo-Australian plate and the Eurasian plate exerts significant influence on seismic activities within the southern seas of Java Island, with potential repercussions extending to the triggering of tsunamis. Given the densely populated nature of this area, especially along the southern region of Yogyakarta Province, the coast of Samas Beach and its surroundings, mitigation efforts are needed to reduce the potential loss of life caused by tsunamis. One of the mitigation efforts is making a tsunami model which can be done using the help of DEMNAS and DEM topographical data from unmanned aerial vehicle (UAV) photogrammetry. The COMCOT software is a tool used in modeling tsunamis based on a numerical model of the shallow water equation that processes tsunami generator parameters and DEM data into an accurate tsunami model. The modeling results show that the tsunami waves will reach the Samas coast in the 38th minute after the occurrence of the earthquake. The maximum height of the tsunami inundation obtained using DEMNAS data was 21.72 m while using the UAV-DEM it was obtained 23.34 m. Comparison of modeling using DEMNAS and UAV-DEM data shows that image data collection using UAV has good resolution and has high accuracy so that it is able to produce a tsunami model that better shows the propagation of a tsunami in the actual field. The location used as a temporary/final evacuation site is Tegalsari Elementary School because of its strategic location and in tsunami modeling, this location is in the very low risk zone.

Keywords: UAV Photogrammetry, COMCOT, Inundation, Evacuation

1. Introduction

Tsunamis are giant waves generated when there is a sudden vertical movement of the seafloor, typically triggered by underwater earthquakes (USGS, 2022). In geosciences, tsunamis are not only generated by earthquakes, but can also be generated by other phenomena that disturb the stability of the sea column such as volcanic eruptions, underwater landslides, cyclones, and the fall of space objects such as meteors (Koshimura et al., 2020). However, according to historical records of tsunamis worldwide in the past, seafloor earthquakes were the ones that most often triggered tsunamis (Atwater et al., 2005).

Widiyantoro et al. (2020) conducted a seismic gap study in the southern region of Java Island by relocating 1,898 earthquakes with Mw ≥ 4.0 from 2009 to 2018 using the teleseismic double-difference technique. The results show a clear longitudinal zone, located between the Java coastline and the Java Trench that exhibits a noticeable absence of seismic activity. Consequently, this region has been identified as a seismic gap. The seismic gap has the potential to become a source of megathrust earthquakes and large tsunamis for the surrounding community.

The seismic gap located south of West Java exhibits a seismic energy deficit equivalent to that of an 8.9 Mw earthquake, assuming a 400-year return period. For the same return period, the high slip deficit area in Central Java and East Java is equivalent to an earthquake with a magnitude of 8.8 Mw, whereas if the two areas rupture in a single earthquake (worst-case scenario) it will result in an earthquake event of 9.2 Mw (Irsyam et al., 2017). Such an earthquake event would likely trigger a tsunami in the southern region of Java Island.

The study location is the coast of Samas Beach, Bantul Regency, an area located on the southern coast of Java which has the potential for earthquakes and tsunamis. This area was once hit by a tsunami that was triggered by the Pangandaran earthquake on July 17, 2006. The earthquake hit the south coast of Yogyakarta with a height of up to 3 m (Triyono et al., 2019). Considering that this area is densely populated and is a tourist destination, mitigation efforts are needed to reduce the number of fatalities caused by the tsunami disaster.

In carrying out tsunami disaster hazard mitigation, making a tsunami hazard map is important for analyzing the vulnerability of an area to a tsunami. Numerical modeling is a solution to produce inundation maps along coastlines that are prone to tsunamis. In this study, the COMCOT (Cornell Multi-grid Coupled Tsunami) modeling code is used to calculate the propagation of the tsunami from the earthquake source to the coastal areas as well as the run-up and inundation of the tsunami. COMCOT adopts explicit staggered leap-frog finite difference schemes to solve shallow water equations (both linear and non-linear). The model's reliability has been confirmed through experimental data (Liu et al., 1995) and has demonstrated successful application in the investigation of several historical tsunami events, such as the 1977 Sumba tsunami (Pradjoko et al., 2015), the 2004 Indian Ocean tsunami (Rasyif et al., 2019; Tursina and Syamsidik, 2019; Wang and Liu, 2007), the 2010 Mentawai tsunami (Hill et al., 2012; Mutmainah et al., 2016) and the Iquique tsunami, Chile 2014 (An et al., 2014).

In COMCOT tsunami modeling, topographical information and tsunami generator parameters are needed (Wang, 2009). To improve the accuracy of modeling, high-resolution topographic data is required. Indonesian Geospatial Agency (BIG) provides topographic data called DEMNAS which has spatial resolution 0.27 arc-second. Another alternative in obtaining topography data is through a combination of photogrammetry and Unmanned Aerial Vehicle (UAV). UAV has several advantages, namely low cost, ability to provide up-to-date data, detailed spatial resolution and specific suitability for topographical mapping in relatively narrow areas (Yan et al., 2010). In this study, the results of the COMCOT tsunami modeling will be compared using topographical data from DEMNAS and DEM (Digital Elevation Model) from the UAV survey for making a map of the tsunami evacuation route on the coast of Samas Beach, Bantul Regency.

2. Methods

2.1 Data Acquisition

Acquisition was conducted in an area of approximately 424 hectares on the coast of Samas Beach, Bantul, Yogyakarta Special Region to obtain aerial photo data using the DJI Mavic Pro 1 drone. Aerial photography is carried out automatically using the Drone Deploy software based on the survey design that has been made. But before the drone flies, it is necessary to calibrate the camera focus, white balance and brightness to avoid bad photo results. The results captured by the UAV are in the form of images or photos with an overlap of 80% and sidelap of 60% between photos. The UAV's flight speed is less than 10 m/s to reduce the possibility of blurry photos. Total flight time is 272 minutes. In one flight the DJI Mavic Pro drone can be airborne for 15-18 minutes including takeoff and landing, so there are 17 flying missions.

Data collection using the UAV was carried out at an average flying altitude of 100 meters above ground level. The photos obtained are integrated with the coordinate points marked on the field which are called Ground Control Points (GCP). GCPs are marked in an "X" shape and installed scattered throughout the area of interest. The coordinates of these points are used to convert the aerial coordinate system to the ground coordinate system for the object being mapped. The GCPs that have been taken will be used for further processing of aerial photographs. Measurement of GCPs was carried out using the fast-static measurement method with reference to WGS 1984 coordinates.

2.2 Structure from Motion

Structure from Motion (SfM) is the process of creating a three-dimensional (3D) representation of an object or scene by analyzing its projection in a sequence of images captured from different viewpoints (Schonberger and Frahm, 2016). SfM uses algorithms to detect matching features within a collection of overlapping digital images (Carrivick et al., 2016).

The SfM process was carried out using the *Agisoft Metashape Professional* software. The process begins with photo alignment, which is the process of finding unique feature points, referred to as "key points", in each image and matching them across the image in pairs to become what are known as "tie points" (Over et al., 2021). Then the GCP coordinates were added to increase the accuracy of alignment coordinates (Over et al., 2021).

After the geometric model has finished, the next step is producing a spatial product which includes:

- Dense cloud built from point clouds.
- DEM, more specifically Digital Surface Model (DSM).
- Orthophoto.

The DEM that will be used in tsunami modeling is the Digital Terrain Model (DTM) so that the DSM resulting from the previous process is converted into DTM by filtering using *PCI Geomatica* software. Terrain filter (flat) is used to remove surface objects so that the original ground elevation (bare earth) is obtained.

Land cover was created using ArcMap software by digitizing land cover features based on their appearance (for example: buildings, trees, etc.) from orthophotos. After obtaining land cover, the value of the Manning roughness coefficient is entered according to the land cover category.

2.3 COMCOT Tsunami Modeling

The tsunami modeling process was executed using the computational program known as the Cornell Multi-Grid Coupled Tsunami Model (COMCOT). COMCOT utilizes explicit staggered leap-frog finite difference schemes for solving the Shallow Water Equations, both in Spherical and Cartesian Coordinates (Wang, 2009). This model incorporates a nested grid system, dynamically linking up to 12 levels (referred to as layers), each with varying grid resolutions. This feature allows for the simulation of tsunamis across different scales. In this study, 4 grid layers are used, where the innermost layer (layer 4) covers the study area on the south coast of Yogyakarta. The data in the first layer (layer 1) uses GEBCO bathymetry data, the second layer (layer 2) uses BATNAS data, the third layer (layer 3) uses DEMNAS data, and the fourth layer (layer 4) uses UAV-DEM and DEMNAS data. The fault parameters used is based on the worst-case megathrust scenario in southern Java which is equivalent to a magnitude of Mw 9.2 based on data from Irsyam et al. (2017).

3. Result and Discussion

To determine the quality of DEM data from UAV aerial photographs, it is necessary to compare it with DEMNAS data. Taking UAV aerial photos until processing to obtain DTM is carried out from February to March 2023, while DEMNAS data is taken from the Geospatial Information Agency (BIG) which was published in 2018. DTM aerial photos UAV has a resolution of 1 m/pixel while DEMNAS data has a spatial resolution 0.27 arc-second (≈8.33 m/pixel). From Fig. 1 it can be seen that DEMNAS with a resolution of 8m/pixel is slightly blurry compared to the DTM UAV which has a resolution of 1m/pixel. The DTM produced by UAV aerial photography has a significant advantage in terms of visual resolution, which will help in increasing the accuracy of tsunami modelling.

Fig. 1 also shows the quite different elevation patterns of the two DEMs. Significant differences can be seen along the coastline where in the DEMNAS data it is not clear that there are sand dunes, while from the DTM UAV it can be clearly seen that there are sand dunes along the coastline. Accuracy was confirmed by direct observations indicating the presence of sandbars along the coastline. Another difference can be seen in the middle of the study area, where in the DTM UAV data from the South to the North the elevation is high, while in DEMNAS the elevation is only high in the North. Field observations show the presence of sand dunes in it.

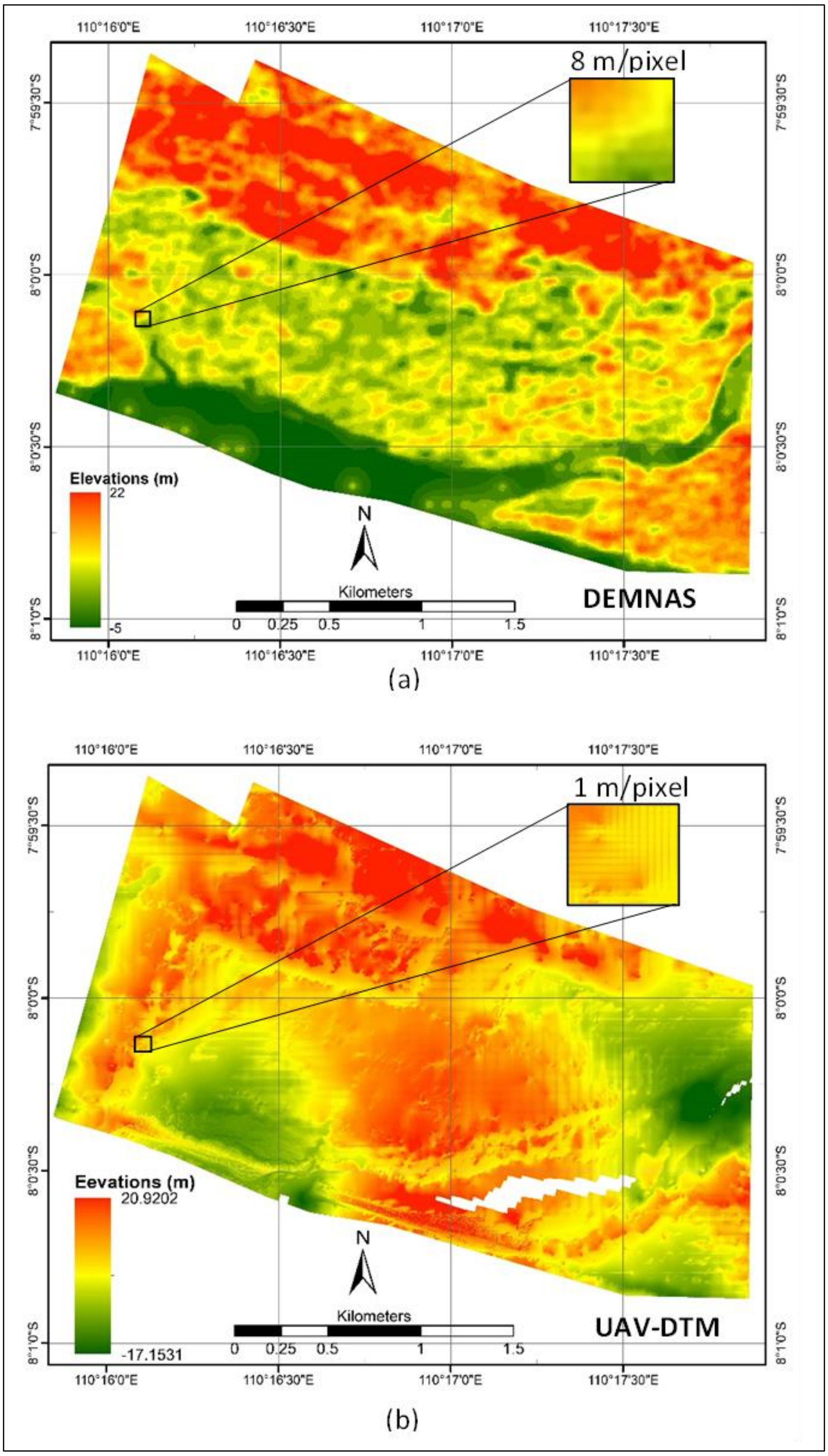

Fig 1. Topography of the study area from (a) DEMNAS (b) UAV-DEM

The modeling results obtained are in the form of a tsunami inundation model and a tsunami wave arrival time. Modeling was carried out for 2 hours with a time change of every 1 minute and the highest altitude estimate for each time was selected during the processing. This modeling time is considered sufficient to visualize the arrival of the tsunami waves to the coast of Samas Beach. In this simulation, the resulting inundation model resolution is 9.2 m/pixel.

The results of tsunami modeling using DEMNAS in the form of a map of the height of the tsunami inundation overlaid with the arrival time of the tsunami waves (Fig. 2) show that the entire study area will be inundated by a tsunami. From Fig. 2, it is known that the tsunami waves will reach the mainland 38-39 minutes after the earthquake occurs. The water level on land can reach 21.72 m, namely in the south of Srigading Village which is a rice field area. Meanwhile, the results of modeling with the UAV-DEM (Fig. 3) show that the water level on land will reach 23.34 with a similar arrival time for tsunami waves, namely 38-39 minutes after the earthquake occurred.

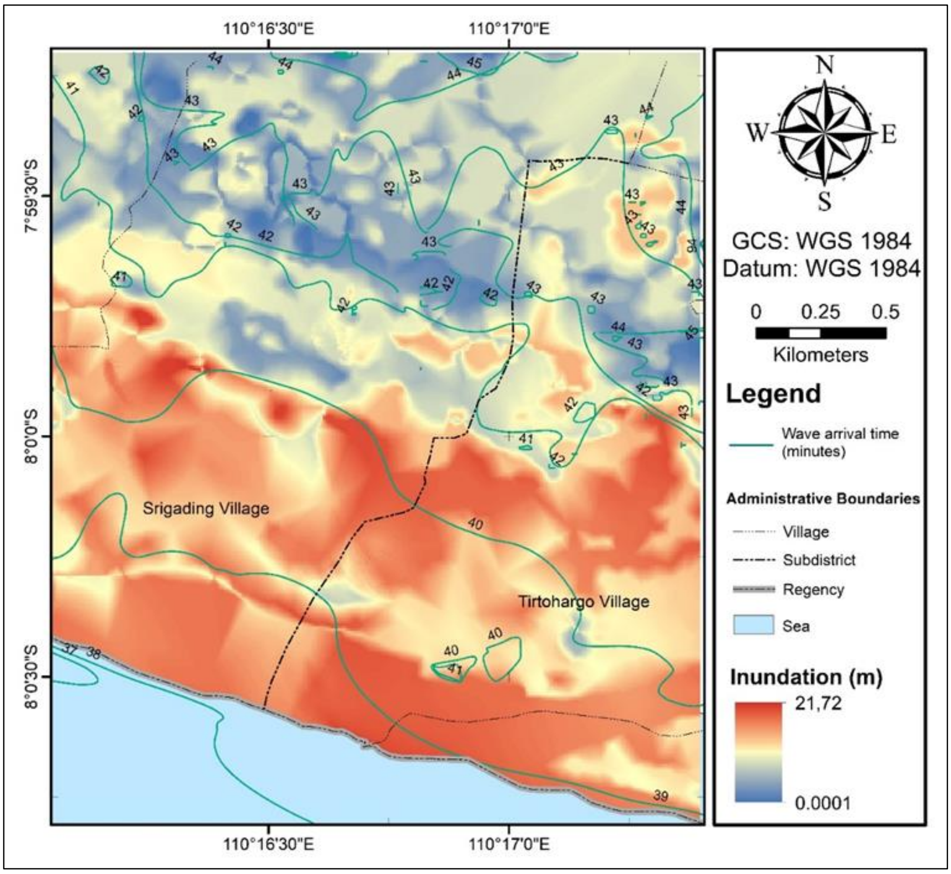

Fig 2. Map of the tsunami inundation height using DEMNAS overlaid with the arrival time of the tsunami waves

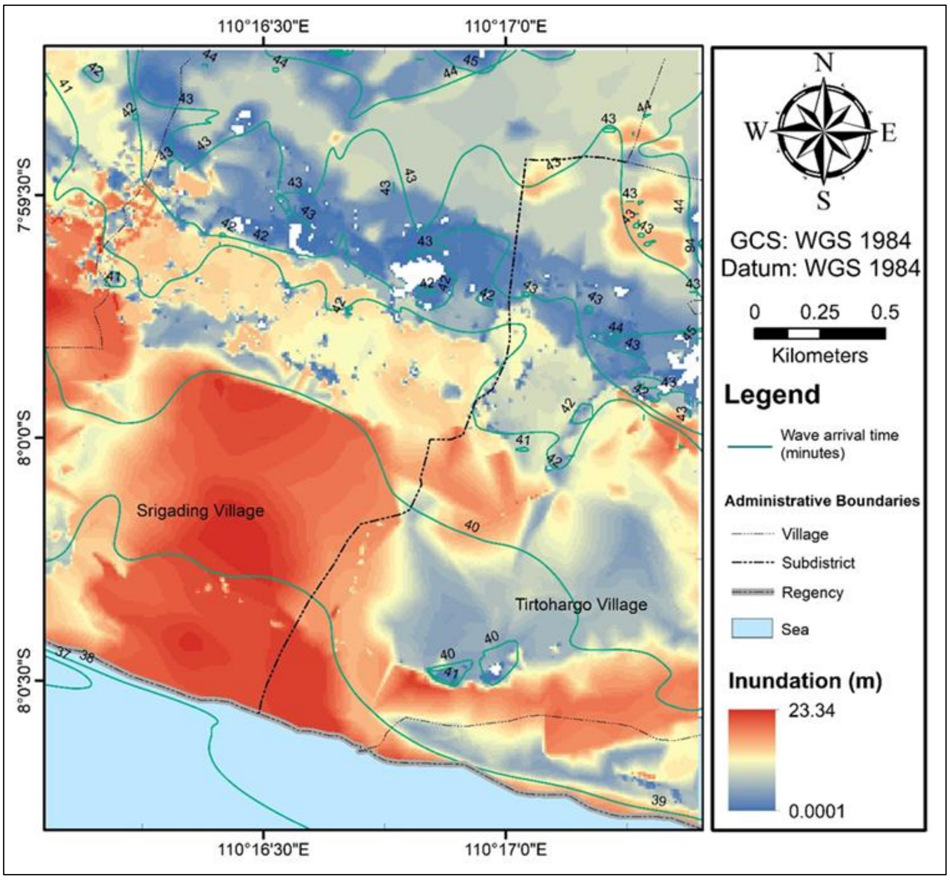

Fig 3. Map of the tsunami inundation height using UAV-DEM overlaid with the arrival time of the tsunami waves

In general, the inundation height is lower in the model results using the UAV-DEM except in the southern area of Srigading Village which is a rice field area. In this area, the level of inundation is more uniform in the simulation results using the UAV-DEM data than the DEMNAS data, which from observations of the rice fields have relatively uniform heights. In the North area, the inundation results using UAV-DEM are lower than using DEMNAS data. In that area there are 3 GPS Geodetic measurement points which show that there is indeed an elevation increase from the height of the rice fields to the south. The area is dominated by residential areas and trees which are obstacles to the passage of tsunami waves. In the south of Titohargo village, the inundation results using UAV-DEM were lower than using DEMNAS data. The results of field checks show that the area is an area of one sand dune located around Samas Beach. These differences show that simulation results using UAV-DEM data which have high resolution and are more up-to-date can provide more accurate results than DEMNAS data. Based on the results, an evacuation route map on the coast of Samas Beach will be made based on tsunami modeling using UAV-DEM data.

Based on the results of the inundation analysis in the observation area to be precise on the coast of Samas Beach, the authors created an evacuation route map which is used as a community guide when a tsunami occurs with the worst scenario in the future to go to the Temporary Evacuation Point (TEP) or Final Evacuation Point (FEP) as shown in Fig. 4. The available TEP/FEP is located at Tegalsari Elementary School (7.993° South Latitude and 110.276° East Longitude) with a height of 15 meters above sea level, because it is in a higher location compared to the modeling results of the tsunami inundation on the coast of Samas Beach. This location is suitable for use as an evacuation site because the location is open, wide and in tsunami modeling the location is in the very low risk zone.

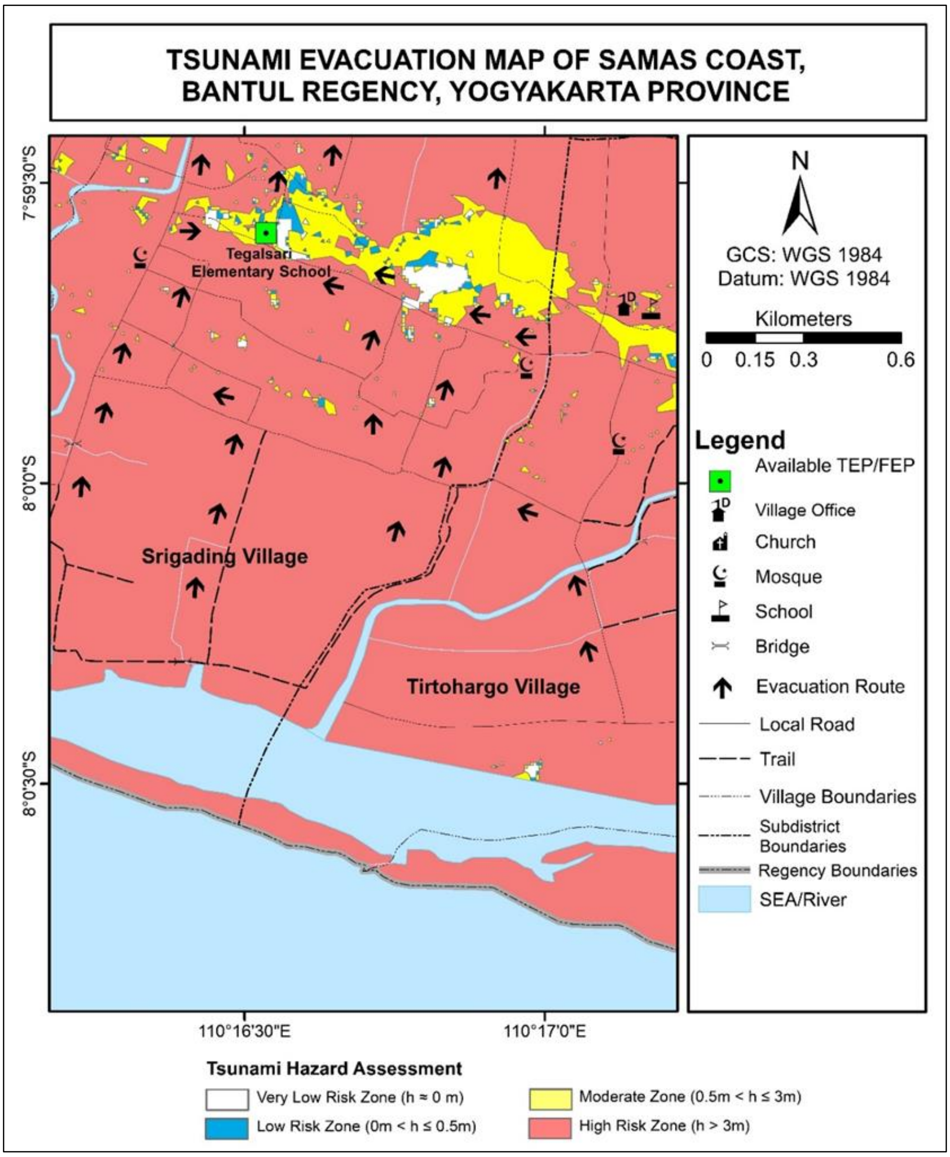

Fig 4. Tsunami Evacuation Map of Samas Coast, Bantul Regency

This study, however, is subject to several limitations. The first is the study area selected is insufficiently expansive. As can be seen in Fig. 4, there is no visible area classified as a very low risk area that is truly extensive. As a result, with this narrow area, there is no place that meets the classification as a Final Evacuation Point. Next, evacuation route planning in this study is only based on the closest route to the Temporary Evacuation Point, without considering other factors such as the number of people affected, evacuation route capacity, topography, etc. These limitations underscore the necessity for future research endeavors to conduct photogrammetric surveys covering a broader expanse and to formulate evacuation route plans that account for multifarious factors inherent in the principles of evacuation route planning.

4. Conclusion

From the tsunami modeling, it is known that the tsunami waves from the worst earthquake scenario in South Java will reach the coast of Samas Beach in the 38th minute after the earthquake occurs. Using DEMNAS data, the maximum tsunami height on the coast of Samas reaches 21.72 meters, while using UAV-DEM data, the maximum tsunami height on the coast of Samas is 23.34 meters. From the comparison of model results it was concluded that the use of UAV-DEM data produces a model that is closer to the actual conditions in the field due to its accuracy, higher resolution, and data updates. Tegalsari Elementary School was chosen as the location for the temporary/final evacuation point because of its strategic location and in tsunami modeling, the location is included in the very low risk zone.

Acknowledgements

The authors are grateful to Gadjah Mada University and BMKG for supporting this study.

References

An, C., Sepúlveda, I., Liu, P.L.-F., 2014. Tsunami source and its validation of the 2014 Iquique, Chile, earthquake. Geophys Res Lett 41, 3988–3994. https://doi.org/10.1002/2014GL060567

Atwater, B., Cisternas, M., Bourgeois, J., Dudley, W., Hendley, J., Stauffer, P., 2005. Surviving a tsunami: Lessons from Chile, Hawaii, and Japan, Circular 1187. US Geological Survey, Reston.

Carrivick, J.L., Smith, M.W., Quincey, D.J., 2016. Structure from Motion in the Geosciences. John Wiley & Sons.

Hill, E.M., Borrero, J.C., Huang, Z., Qiu, Q., Banerjee, P., Natawidjaja, D.H., Elosegui, P., Fritz, H.M., Suwargadi, B.W., Pranantyo, I.R., Li, L., Macpherson, K.A., Skanavis, V., Synolakis, C.E., Sieh, K., 2012. The 2010 M_w 7.8 Mentawai earthquake: Very shallow source of a rare tsunami earthquake determined from tsunami field survey and near- field GPS data. J Geophys Res Solid Earth 117. https://doi.org/10.1029/2012JB009159

Irsyam, M., Widiyantoro, S., Natawidjaja, D.H., Meilano, I., Rudyanto, A., Hidayati, S., Triyoso, W., Hanifa, N.R., Djarwadi, D., Faizal, L., Sunarjito, 2017. Peta Sumber dan Bahaya Gempa Indonesia Tahun 2017, 1st ed. Pusat Penelitian dan Pengembangan Perumahan dan Permukiman, Bandung.

Koshimura, S., Moya, L., Mas, E., Bai, Y., 2020. Tsunami Damage Detection with Remote Sensing: A Review. Geosciences (Basel) 10, 177. https://doi.org/10.3390/geosciences10050177

Liu, P.L.-F., Cho, Y.-S., Briggs, M.J., Kanoglu, U., Synolakis, C.E., 1995. Runup of solitary waves on a circular Island. J Fluid Mech 302, 259–285. https://doi.org/10.1017/S0022112095004095

Mutmainah, H., Christiana, D.W., Kusumah, G., 2016. Tsunami Mentawai 25 Oktober 2010 (Simulasi Comcot 1.7) Dan Dampaknya Kini Terhadap Pantai Barat Mentawai. Jurnal Kelautan: Indonesian Journal of Marine Science and Technology 9, 175. https://doi.org/10.21107/jk.v9i2.1917

Over, J.-S.R., Ritchie, A.C., Kranenburg, C.J., Brown, J.A., Buscombe, D.D., Noble, T., Sherwood, C.R., Warrick, J.A., Wernette, P.A., 2021. Processing coastal imagery with Agisoft Metashape Professional Edition, version 1.6—Structure from motion workflow documentation.

Pradjoko, E., Kusuma, T., Setyandito, O., Suroso, A., Harianto, B., 2015. The Tsunami Run-up Assesment of 1977 Sumba Earthquake in Kuta, Center of Lombok, Indonesia. Procedia Earth and Planetary Science 14, 9–16. https://doi.org/10.1016/j.proeps.2015.07.079

Rasyif, T., Kato, S., Syamsidik, Okabe, T., 2019. Numerical Simulation of Morphological Changes due to the 2004 Tsunami Wave around Banda Aceh, Indonesia. Geosciences (Basel) 9, 125. https://doi.org/10.3390/geosciences9030125

Schonberger, J.L., Frahm, J.-M., 2016. Structure-From-Motion Revisited, in: Proceedings of the IEEE Conference on Computer Vision and Pattern Recognition (CVPR).

Triyono, R., Prasetya, T., Daryono, Anugrah, S.D., Sudrajat, A., Setiyono, U., Gunawan, I., Priyobudi, Yatimantoro, T., Hidayanti, Anggraini, S., Rahayu, R.H., Yogaswara, D.S., Hawati, P., Apriani, M., Julius, A.M., Harvan, M., Simangunsong, G., Kriswinarso, T., 2019. Katalog Tsunami Indonesia Tahun 416-2018. Badan Meteorologi Klimatologi dan Geofisika, Jakarta.

Tursina, Syamsidik, 2019. Reconstruction of the 2004 Tsunami Inundation Map in Banda Aceh Through Numerical Model and Its Validation with Post-Tsunami Survey Data. IOP Conf Ser Earth Environ Sci 273, 012008. https://doi.org/10.1088/1755-1315/273/1/012008

USGS, 2022. Tsunamis [WWW Document]. URL https://www.usgs.gov/special-topics/subduction-zone-science/science/tsunamis (accessed 5.24.23).

Wang, X., 2009. User manual for COMCOT version 1.7 (first draft). Cornel University 65.

Wang, X., Liu, P.L.-F., 2007. Numerical Simulations of the 2004 Indian Ocean Tsunamis — Coastal Effects. Journal of Earthquake and Tsunami 01, 273–297. https://doi.org/10.1142/S179343110700016X

Widiyantoro, S., Gunawan, E., Muhari, A., Rawlinson, N., Mori, J., Hanifa, N.R., Susilo, S., Supendi, P., Shiddiqi, H.A., Nugraha, A.D., Putra, H.E., 2020. Implications for megathrust earthquakes and tsunamis from seismic gaps south of Java Indonesia. Sci Rep 10, 15274. https://doi.org/10.1038/s41598-020-72142-z

Yan, L., Gou, Z., Duan, Y., 2010. A UAV Remote Sensing System: Design and Tests, in: Geospatial Technology for Earth Observation. Springer US, Boston, MA, pp. 27–44.https://doi.org/10.1007/978-1-4419-0050-0_2